Dynamic Ionosphere Cubesat Experiment (DICE)

Geoff Crowley
ASTRA
11118 Quail Pass, San Antonio, TX 78249; 210-834-3475
gcrowley@astraspace.net

Chad Fish, Charles Swenson, Robert Burt and Tim Neilsen
Space Dynamics Lab/USURF
1695 North Research Park Way, North Logan, UT 84341; 435-797-0496; 435-797-2958
chad.fish@sdl.usu.edu; charles.swenson@usu.edu

Aroh Barjatya
Embry-Riddle Aeronautical University
600 S. Clyde Morris Boulevard, Daytona Beach, FL 32114-3900; 386-226-6675
barjatya@erau.edu

Gary Bust
ASTRA
11118 Quail Pass, San Antonio, TX 78249; 512-947-2689
gbust@astraspace.net

Miguel Larsen
Clemson University
118 Kinard Laboratory, Clemson, SC 29634-1911; 864-656-5309
mlarsen@clemson.edu

ABSTRACT

The Dynamic Ionosphere Cubesat Experiment (DICE) mission has been selected for flight under the NSF "CubeSat-based Science Mission for Space Weather and Atmospheric Research" program. The mission has three scientific objectives: (1) Investigate the physical processes responsible for formation of the midlatitude ionospheric Storm Enhanced Density (SED) bulge in the noon to post-noon sector during magnetic storms; (2) Investigate the physical processes responsible for the formation of the SED plume at the base of the SED bulge and the transport of the high density SED plume across the magnetic pole; (3) Investigate the relationship between penetration electric fields and the formation and evolution of SED.

The mission consists of two identical Cubesats launched simultaneously. Each satellite carries a fixed-bias DC Langmuir Probe (DCP) to measure in-situ ionospheric plasma densities, and an Electric Field Probe (EFP) to measure DC and AC electric fields. These measurements will permit accurate identification of storm-time features such as the SED bulge and plume, together with simultaneous co-located electric field measurements which have previously been missing. The mission team combines expertise from ASTRA, Utah State University/Space Dynamics Laboratory (USU/SDL), Embry-Riddle Aeronautical University and Clemson University.

1. INTRODUCTION

Space weather refers to conditions in space (the Sun, solar wind, magnetosphere, ionosphere, or thermosphere) that can influence the performance and reliability of space-borne and ground-based technological systems. Ionospheric variability has a particularly dramatic effect on radio frequency (RF) systems; for example, large gradients in ionospheric electron density can impact communications, surveillance and navigation systems [Skone et al., 2004; Sojka et al., 2004; Sparks et al., 2004; Basu et al., 2005]. Some of the largest gradients are found on the edges of Storm Enhanced Density (SED) features, which regularly occur over the US in the afternoon during magnetic disturbances. The SED feature was first identified by Foster [1993] using the Millstone Hill incoherent scatter radar (ISR), although Total Electron Content (TEC) enhancements caused by SEDs had been

observed much earlier [*Klobuchar et al.*, 1968, 1971; *Mendillo*, 2006]. More recently, 2-D TEC maps obtained from global ground GPS receivers have shed new light on the space-time properties of mid latitude SED, and its relationship to plasmaspheric processes [*Foster et al.*, 2002; *Coster et al.*, 2003; *Foster and Rideout*, 2005].

The formation and evolution of SED can be described by two related structures (reference Figure 1). The first is the formation of a greatly enhanced SED "bulge" of plasma [*Foster et al., 2005*; *Foster and Coster*, 2007; *Mannucci et al.*, 2007] which seems to preferentially originate at southern USA latitudes and appears correlated with storm-time prompt penetration electric fields (PPE) at low latitudes. The second is the formation and evolution of a narrow SED "plasma plume" that first forms at the base of the SED bulge, and then extends pole-ward into and across the polar cap. The SED plume appears to be strongly correlated with the expansion of the polar convection cells, and is thought by some investigators to be due to the existence of a strong sub-auroral polarization stream (SAPS) in the local afternoon/evening mid-latitude sector [*Foster and Vo*, 2002; *Foster and Rideout,* 2005; *Foster et al.*, 2007].

the F-region peak electron density (not TEC) distribution from IDA4D for the SEDs observed in the afternoon mid-latitude American sector during super-storms on October 30 and November 20, 2003. The SED for the two storms have similar characteristics, most notably with both cases forming in the post-noon period across the USA. However, the details of the structures between the two SED are quite different. The most striking feature of contrast between the two storms is the location and orientation of formation of the high-density plasma bulge and the orientation of the narrow plume of plasma or tongue of ionization (TOI) associated with each bulge. For the October storm, the high-density plasma bulge forms off the west coast of the USA and Mexico, with the general bulge orientation aligned with the Californian and Mexican coastline. The associated TOI stretches in a southwest to northeast direction up over the pole. For the November storm, the bulge forms off the southeastern coast of the USA in the Caribbean. The associated TOI stretches from the southeast to northwest towards the pole. Additionally, the SED bulge for the October storm extends to higher latitudes (approximately 45°) than for the November storm (approximately 35°). Note that both events are located between local noon and the terminator (18LT).

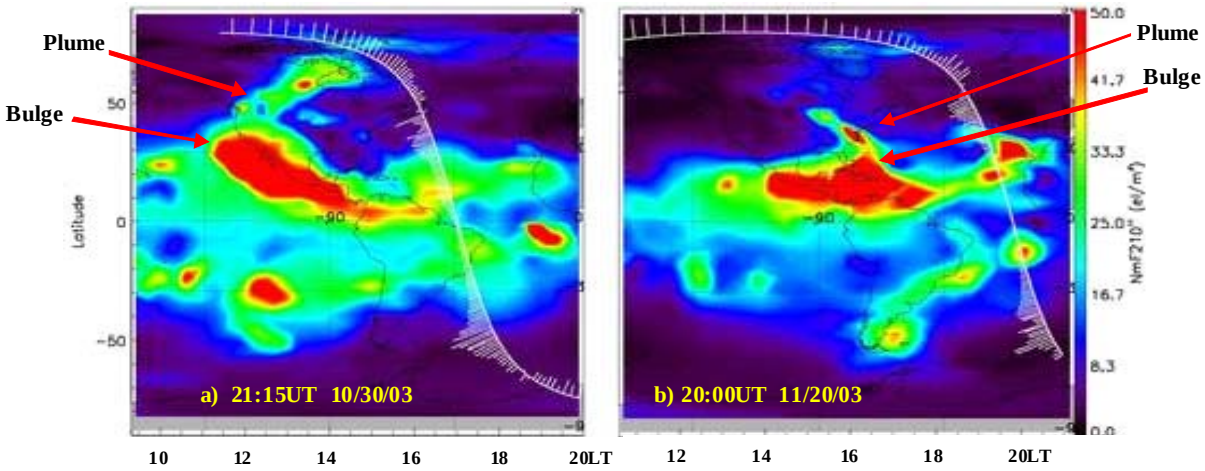

Figure 1. Horizontal distribution (Latitude vs. Local Time) of F-region peak electron density (NmF2) from IDA4D for: (a) October 30 (b) November 20, 2003. Units are 1.e11 m-3. DMSP ion drift vectors shown.

Recently, Bust [2008] and Bust et al. [2008a, 2008b] have studied the SED bulge and plume development using an assimilative technique called Ionospheric Data Assimilation Algorithm 4-Dimensional (IDA4D) that ingests many different kinds of electron density-related data [Bust et al., 2004]. The advantage of IDA4D over the previous TEC analyses is that IDA4D provides the 3-D electron density distribution rather than just the 2-D TEC distribution. For example, Figure 1 compares

IDA4D also provides vertical slices [Bust et al., 2008] that can be used to investigate the relationship between the onset of PPE, the growth and separation of the equatorial anomalies, and formation and evolution of the SED. Figure 2 (panels c-h) shows a sequence of 6 such vertical slices at 250º longitude for the October 30 storm, from local times of 1040-1540LT. For comparison, two corresponding images from a quiet day are shown in panels a and b. Panel f at 1340LT corresponds to a slice through Figure 1a.

In panels c-h of Figure 2, one can clearly identify a separation of the anomaly peaks, a sharpening of the horizontal gradient of plasma along with the distribution of plasma to high altitudes at the poleward edge of the SED, and finally a separation and growth of the SED components near 50-60ºN. Note that all of these features occurred in the 1340-1540 LT sector. Analysis of the November storm identifies similar formation and evolution characteristics, with the interesting exception that very little altitude uplift of the bulge and plume occurred. None of the SED features occur on the quiet day.

When contrasting the similarities and differences between the formation, evolution and decay of SED for the October and November storms it would be useful to start with the time history of the equatorial vertical drifts. Unfortunately, these are not usually available because DMSP does not fly through the afternoon local times where the SEDs are formed and evolve. What is usually available is an estimate of the equatorial electric field over Jicamarca, occasionally from the Jicamarca incoherent-scatter (IS) radar (does not operate routinely), or obtained from the magnetometer method developed by Dave Anderson and colleagues [*Anderson et al.*, 2002, 2004, 2006]. Occasionally, there are also electric field measurements from the Millstone Hill IS radar. Figure 3 shows the vertical drifts for the two storms using Anderson-derived drifts. For both storms, the initial PPE enhancements at Jicamarca began near local noon. However, there are significant differences in the drift variations for the two storms, including their magnitude and their temporal variation. In the October storm (black curve) the vertical drift reaches peak velocity at about 1300 LT, while for the November storm (red curve), it reaches peak velocity at about 1130 LT. In both cases, the enhancement in vertical drift above climate persists until about 1700 LT (where the Anderson method fails).

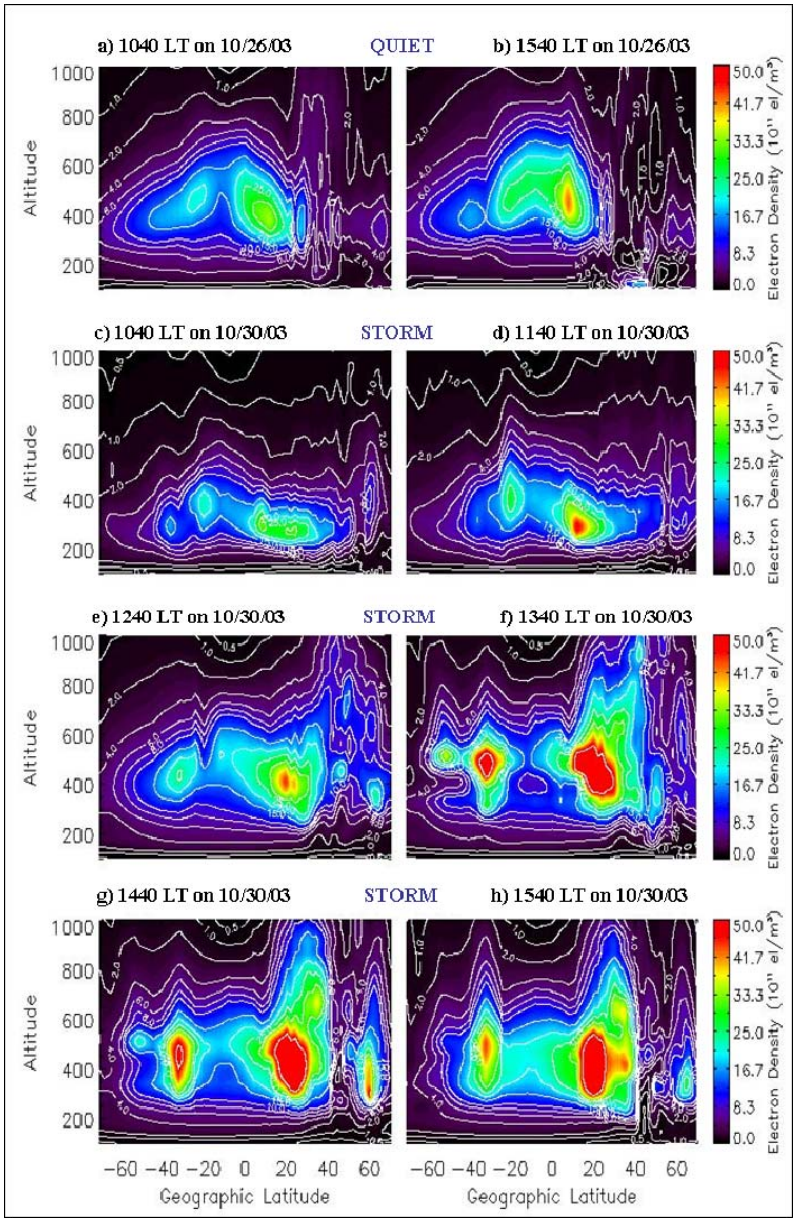

Figure 2. IDA4D slices of electron density (latitude versus altitude) through a constant geographic longitude of 250º for (a-b) Snapshots at 1040 and 1540 LT during a quiet day prior to Oct 30, 2003 storm; (c-h) Sequence from 1040 to 1540LT during the October 30, 2003 storm.

While there appears to be a strong linkage between the appearance of PPE, the growth and separation of the equatorial anomalies, development of an SED mid-latitude bulge, and subsequent formation of TOI (Figures 1-3), the details of that linkage, and how it varies for different storms still requires significant investigation. In addition to the direct investigation of the daytime formation of the SED bulge and plume, there seems to be a relationship between the storm-induced SED that occurs in the noon/post-noon sector, and a plasma enhancement feature observed near and after sunset in the southeastern USA region on October 30-31, 2003 [Bust et al., 2008c]. It is not clear whether there is linkage between the physics of the formation and evolution of the SED feature, and the effect in the

post-sunset ionosphere, or whether the evening enhancement is simply a fossil remnant of the earlier feature.

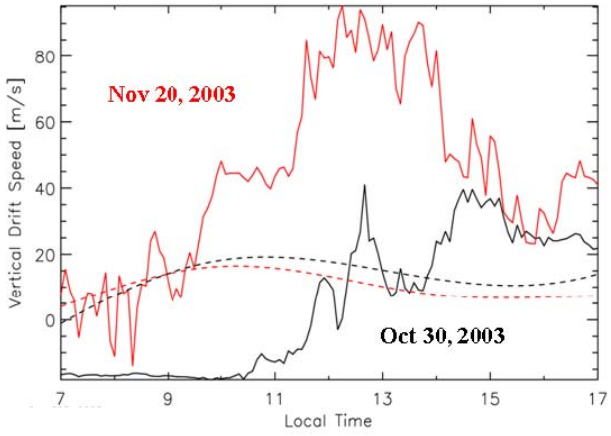

Figure 3. The equatorial vertical drifts for October 30, 2003 (black curve) and November 20, 2003 (red curve) storms (estimated by the method developed by Anderson et al.). Broken lines indicate corresponding quiet day curves from Fejer & Scherliess model.

The DICE mission will provide insight and measurements for further understanding of the formation, evolution, and decay of SED and their related impact on space weather forecasting. In particular, the mission will provide simultaneous key electric field and electron density measurements in the early afternoon sector where many of these events seem to form (see Figs 1-2). Currently, a lack of afternoon sector electric field measurements exists. For example, Figure 4 demonstrates that the sun-synchronous DMSP orbits are at local times that are not able to make SED co-incident measurements. The DICE mission will focus on local times between about 12-16 LT, complementing the DMSP data and together provide dayside electric field measurements across a broad swath of local times.

2. SCIENTIFIC OBJECTIVES

To address the outstanding questions of SED science, the proposed research has three main scientific objectives:

1. Investigate the physical processes responsible for formation of the SED bulge in the noon to post-noon sector during magnetic storms: One of the outstanding questions regarding SED is the detailed mechanisms associated with bulge formation over the southern USA. From the analysis presented in section 1.1.1, this formation process appears to be an extension of the equatorial anomaly region. However, during SED formation, the peak plasma density can double (from 2.5-5.0 $*10^{12}$ e/m^3) within 30 minutes (which is very atypical for common equatorial anomaly). Exactly how such high electron density and TEC (> 200 TECU) form over the southern USA during severe magnetic storms is still an open question. It has been thought that transport of equatorial plasma was the cause of the electron density increase, but the equatorial anomalies do not move to USA latitudes, so there must be additional processes at work. By directly measuring electric fields and electron density in the F-region of the ionosphere during the time periods when the SED bulge forms, we can achieve a greater understanding of the processes producing the bulge.
2) Investigate the physical processes responsible for the formation of the SED plume at the base of the SED bulge and the

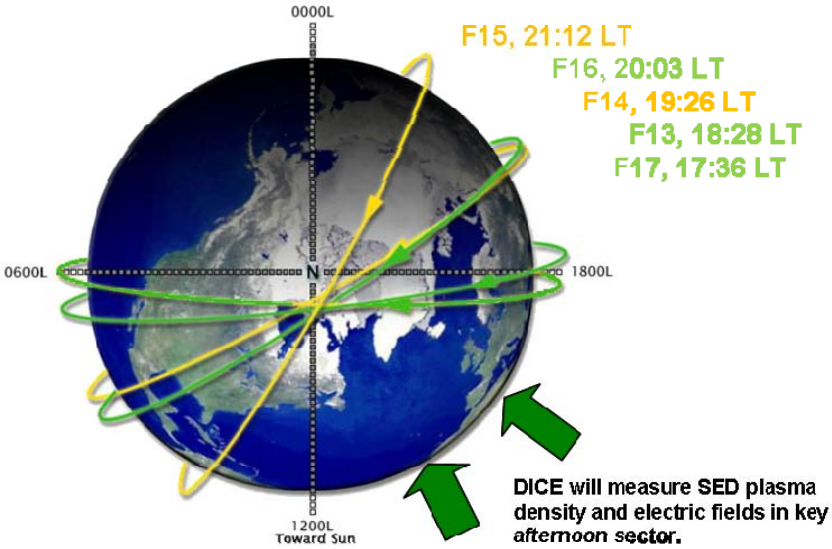

Figure 4. Air Force DMSP satellites are in sun-synchronous orbits that favor the evening and morning hours for operational reasons. The DICE mission will sample local times where SED bulge and plume tend to occur.

transport of the high density SED plume across the magnetic pole: A narrow plume of high density plasma forms out of the bulge and flows towards the polar region at high velocity (> 500 m/s). Thus, a second outstanding question relates to how the mid-latitude SED bulge, which is not moving at high speed, transforms into a tongue-like plume moving poleward at large plasma velocities. In particular, what role do electric fields play, and what is the relationship between an expanded 2-cell convection pattern and Sub-Auroral Polarization Streams (SAPS) fields?

3) Investigate the relationship between PPE and the formation and evolution of SED: The low latitude electric fields are comprised of three components: the quiet-time dynamo, the disturbance dynamo, and the PPE. The DICE spacecraft measures the sum of these electric fields. The use of storm-simulation models, such as the first principles Thermosphere Ionosphere Mesosphere Electrodynamic General Circulation Model (TIMEGCM) will allow an estimate of the disturbance dynamo contribution, based on the storm-time winds. Model post-processors will permit the model wind dynamo to be computed separately from the PPE. Recent work has demonstrated the capability of the TIMEGCM, located at ASTRA, to predict PPE at the equatorial region during severe magnetic storms [*Crowley and Kelley*, 2008]. Comparison of the measured ion drift speed at Jicamarca with the values predicted by the TIMEGCM, reveals that the TIMEGCM predicts many of the gross features of the PPE when driven by high latitude potentials from AMIE (Assimilative Mapping of Ionospheric Electrodynamics). The TIMEGCM model ionosphere responds to these electric fields, resulting in changes of the position and intensity of the Appleton Anomaly peaks. However, the TIMEGCM resolution of 5º is too coarse to accurately simulate SEDs. The DICE plasma and electric field measurements will be compared with TIMEGCM model simulations to better understand and quantify the relationship between the occurrence of PPE at the equator, the growth and separation of the Appleton anomaly peaks, and the formation of the SED bulge. The model will also provide a 1st-order estimate of the role of winds and composition in the plasma variations [e.g. *Crowley et al*., 2006].

3. SCIENCE MEASUREMENT(S) AND REQUIREMENT(S)

The DICE science objectives will be achieved via *in-situ* ionospheric electrical field and plasma density measurements from a two-spacecraft constellation. The electric field and plasma density measurements will allow for the characterization of both the ionospheric plasma density and the electric field distribution. The general SED plasma density and electric field characteristics were illustrated by Figures 1-3. Ideally what is needed to study SEDs is a set of simultaneous co-located plasma density and electric field measurements passing through the SED bulge and plume **in the afternoon sector** as they start to develop and then as they evolve. As shown in Figure 4, DMSP is almost never in the appropriate local time (LT) sector to see the afternoon development, although features near 18LT can be studied with DMSP. Thus the DICE satellites should sample the afternoon sector between 12-16LT, where they will observe important features that have never been seen by DMSP. With two DICE spacecraft, it will be possible to begin to separate temporal and spatial evolution of the SEDs. The two DICE spacecraft will drift apart in latitude over the life of the mission, so that they see the same plasma at slightly different times (time evolution). It would also be useful to have the DICE spacecraft orbits differing by 1-3 hours in LT. Although it is expected that this longitudinal variation will not be possible to implement on the 6-month DICE mission alone, the DMSP satellite data will be collected at LT separated by up to several hours from DICE, thus making the DMSP-DICE synergism extremely valuable. A sun-synchronous DICE orbit in the 12-16LT range would be ideal, but not a requirement.

SEDs are large-scale features; therefore high time-resolution is not required for the DICE measurements. Figures 1 and 2 show that the SED plume is about 500-1000 km wide, while the bulge and the Appleton Anomalies are even wider. The electric fields causing the SED bulge and plume have similar scales. With an approximate spacecraft velocity of 7 km/sec a DICE spacecraft will take approximately 7-14 seconds to traverse the SED plume, therefore a cadence of 0.5 to 1 seconds for the plasma and electric field measurements is sufficient to define the SED plume and the related (broader) plasma electric field structures. Although not the focus of the DICE mission, ionospheric irregularities are of great interest for space weather. Further, it has been shown [*Basu et al.*, 2005] that small scale irregularities form on the edges of large SED gradients. The physical instability mechanism is not known, so directly measuring small scale electric fields in association with larger scale SEDs will be quite valuable. The irregularity spectrum will also be

captured by the DICE mission in terms of the AC electric field spectrum measurements. In addition, observations at the Millstone Hill ISR [*Foster et al.*, 2004; *Ericson et al.*, 2002] have shown small scale electric field variability associated with the larger scale SAPS channel. It is possible that there is a physical connection between small scale AC electric field variability and the larger scale dynamics of the SED plume development right on the edge of the large scale gradient field. The expected launch of the DICE mission is no sooner than 2011, following the start of the rise in solar activity for the next cycle. Therefore, the plasma instruments will have no trouble with light ions, such as they might experience at solar minimum. The level of geomagnetic activity will also increase with solar activity, resulting in typically at least one SED per month. Therefore a 6-month mission will be sufficient to observe a number of SEDs and penetration E-field events.

Table 1 provides the science objectives to mission functional requirements traceability listing. Section 1.3 contains a comprehensive description of the orbital requirements for the mission.

Table 1. Science to Mission Functionality Requirements Traceability Matrix

Science Objective 1: Investigate formation of the SED bulge over the USA		
Measurement Req	**Instrument Req**	**Mission Req**
Measure RMS Fluctuations in Electric Field and Plasma Density: 1. Make co-located DC electric field and plasma density measurements at a ≤ 10 km on-orbit resolution 2. Make AC electric field measurements at a ≤ 10 km on-orbit resolution 3. Make measurements on a constellation platform of ≥ 2 spacecraft that are within 300 km	**Electric Field**: 1. Max range of ± 0.6 V/m 2. Min threshold of 0.6 mV/m 3. Min resolution of 0.15 mV/m 4. DC sample rate ≥ 4 Hz 5. AC sample rate ≥ 4 kHz [Telemeter AC FFT power information at ≥ 1 Hz (3 points)] **Plasma (Ion) Density**: 1. Range of $2x10^{9}$-2 $x10^{13}$ m^{-3} 2. Min resolution of 3 $x10^{8}$ m^{-3} 3. Sample rate ≥ 1 Hz	1. Constellation size ≥ 2 satellites 2. Spacecraft spin ≥ 0.8 Hz 3. Spacecraft spin axis aligned to geodetic axis to within 10 º (1σ) 4. Spacecraft spin stabilized to within 1º (1σ) about principal spin axis 5. Spacecraft knowledge to within 1º (1σ) 5. Constellation time synch knowledge ≤ 1 s 6. Orbital insertion inclination between 55 - 98 º (ideally sun-synchronous at 12-16LT) 7. Orbital altitude between 350 - 630 km 8. 'Circular' orbits (eccentricity of ≤ 0.2) 9. Spacecraft delV speed of ≤ 50 km/month 10. Storage/downlink ≥ 31 Mbits/day. 11. Lifetime ≥ 6 months
Science Objective 2: Investigate formation of the SED plume over the USA		
Measurement Req	**Instrument Req**	**Mission Req**
Same as Science Objective 1	Same as Science Objective 1	Same as Science Objective 1 (downlink included in Objective 1)
Science Objective 3: Investigate correlation of PPE with formation and evolution of SED		
Measurement Req	**Instrument Req**	**Mission Req**
Same as Science Objective 1	Same as Science Objective 1	Same as Science Objective 1 (downlink included in Objective 1)

4. INSTRUMENTATION DESIGN

4.1 Spacecraft Configuration and Orbital Orientation: The DICE science objectives will be achieved via *in-situ* ionospheric electric field and plasma density measurements. The measurements will be made using two instruments; the Electric Field Probe (EFP) for electric field measurements and the fixed-bias DC Langmuir Probe (DCP) for absolute ion density measurements. These instruments draw on more than 20 years of sounding rocket and orbital flight heritage at USU/SDL. Recent missions that have successfully used these types of instruments including the Floating Potential Measurement Unit (FPMU) [2005] program on the International Space Station (ISS), and the Tropical Storm [2007] and EQUIS II [2005] sounding rocket programs. Both instruments are tightly integrated with the DICE spacecraft design. Figure 5 shows the DICE spacecraft and instrumentation configuration. Each of the two DICE spacecraft is identical in design and function. The two EFP booms (pale blue) extend 2 m each away from the spacecraft with spheres on the ends of the booms. The other two booms are for UHF communications and are 0.9 m in length each (only part of the length is metallic material for the antenna; the rest is a dielectric material). The UHF booms also provide balance for the controlled spin of the spacecraft. The DCP sensor spheres are supported on the top and bottom of the spacecraft by fiberglass booms that extend 5 cm. The electronics for the EFP and DCP are housed in the spacecraft on the science board.

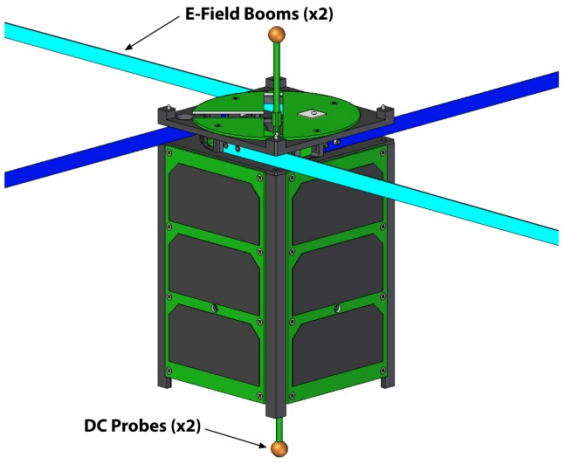

Figure 5. DICE spacecraft and sensor suite.

Both DICE spacecraft will be inserted jointly into orbit from a P-POD. The lead DICE spacecraft will have an approximate 6 mm/s deltaV imposed upon it to create separation between the two spacecraft along the velocity vector. Over a period of 6 months, the along-track (velocity vector) separation between the spacecraft will grow to approximately 300 km. The EFP, UHF antenna dipole, and DCP booms will be deployed by each spacecraft after launch, using a pre-determined commissioning sequence that ensures a safe inter-spacecraft separation distance prior to antenna deployment. The spacecraft will then continue with the commissioning sequence, which will include a 1 Hz spacecraft spin-up stabilization event that is autonomously controlled by the spacecraft ADCS system.

The spacecraft spin stabilization will provide two-dimensional measurements of the electric field at 1 Hz, and thus allow a deterministic ground processing removal of the $\boldsymbol{v} \times \boldsymbol{B}$ induced electric field component that is superimposed upon the target environmental electric field due to spacecraft movement through the geomagnetic field (also see Figure 6). The worst case $\boldsymbol{v} \times \boldsymbol{B}$ induced electric field component is expected to be on the order of 350 mV/m, while the quiet time environmental EFP measurement capability is expected to be on the order of 0.5 mV/m. Therefore, the process of systematically determining the $\boldsymbol{v} \times \boldsymbol{B}$ electric field from the sinusoidal measurement created by the spin of the spacecraft is critical in removing the induced field component from the total measurement during data analysis. In addition, accurate knowledge of the spacecraft attitude (within 1°, 1σ) is important in determining the contribution of the induced field to the total measurement. The minimum EFP electric field measurement capability of 0.5 mV/m is a typical equatorial quiet time value. Storm-time electric fields associated with SEDs are several times larger. The 0.5 mV/m measurement threshold is limited by such features as the sensor surface work function and the local environment created by the wake of the spacecraft. Thus, the EFP booms have been designed to extend to distances much greater than the spacecraft structure size. While the electric field threshold is conservatively expected to be 0.5 mV/m, the resolution is much finer at 100 μV/m. Post-mission processing may enable a threshold smaller than 0.5 mV/m to be obtained.

The DICE spacecraft orbital orientation is shown in Figure 6. Each DICE spacecraft will spin with the spacecraft z-axis (long axis) aligned to ≤ 5° (1σ) of the inertial J2000 z-axis. This orbital orientation facilitates the measurement of the electric field component orthogonal to the geomagnetic field over a majority of the orbit. Additionally, this orbital orientation ensures a purely spherical projection of the DCP sphere into the spacecraft ram direction with only minor effect from the cylindrical boom at high latitudes. Post-processing will determine spacecraft attitude to much less than 1°

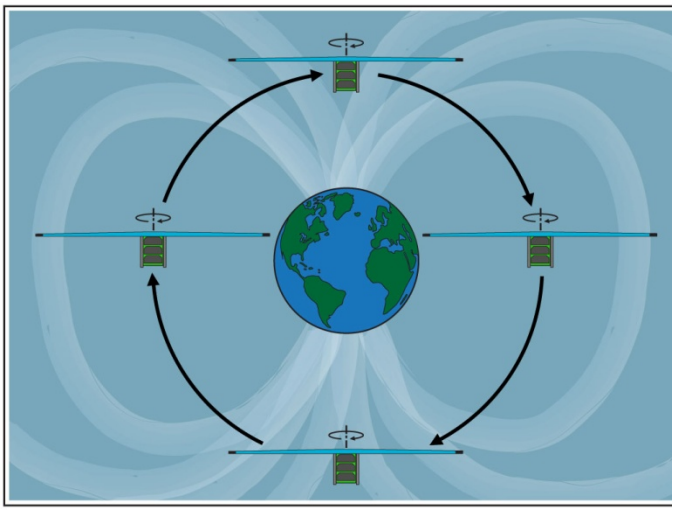

Figure 6. Spacecraft orbital orientation.

(1σ, 3-axis). On-board GPS measurements will also provide daily navigational updates accurate to within 1 μs and 10 meters.

4.2 Electric Field Probe (EFP): The EFP is an implementation of the double-probe class of *in-situ* electric field instruments. It includes two metallic two-meter booms that will extend into the plasma environment from opposite sides of the spacecraft (ref. Figure 5). A majority of the length of each boom is electrically insulated from the plasma environment by germanium-coated kapton tape, with small spheres (0.5 cm diameters) on each boom tip exposed to plasma. The germanium coating mitigates charge build-up on the insulated boom sections. The exposed boom tips are gold-plated to minimize geometric work function dissimilarities. The input resistance of the boom sensor electronics is greater than 10^{15} Ω, which eliminates large instrument-induced offset voltages being superimposed upon the targeted environmental measurement. The sensor electronics measure the boom tip voltage at a resolution of ≤100 μV/m over a range of ±1 V/m.

The EFP makes both DC and AC electric field measurements. The DC measurements are made at equal time steps and telemetered at an 8 Hz rate, thus providing 45° rotational resolution per spacecraft spin and maximizing science return. Oversampling and decimation of the DC signal occurs on-board to improve both signal to noise ratio and to create a characterized filter for the sampled data. The DC measurements are a subset of the AC measurements and co-incident with the AC measurements. The AC measurements are sampled at 4096 Hz in equal time steps. The AC measurements are processed on-board through a FFT algorithm. The resultant magnitude of three distinct frequencies can then be telemetered at 1 Hz for ground analysis. The three frequencies selected are: (50, 1300, 2048 Hz). The first frequency corresponds to the Fresnel scale for GPS (200-300 meters), while the latter sample rate enables resolution of electric field structures that are < 3.5 m. The middle value provides some idea of the spectral shape.

While not the primary science mission, the AC field measurements will contribute to the overall scientific success of the mission in two ways. First, it is known [*Basu et al.*, 2005] that small-scale density irregularities form at the edges of the SED plumes. What is not known is the exact physical mechanism that produces the irregularities. It could be a gradient-drift instability, which would only involve large scale DC fields. However, it could also be related to a Farley-Buneman instabilities or Kelvin-Helmholtz instabilities. Making coincident measurements of the small scale fluctuating electric field, electron density fluctuations and the larger scale fields in the presence of SED instabilities will provide new insight into the instability mechanisms. The second way the AC field measurements will contribute to the science is in adding to our overall understanding of the micro-scale and meso-scale physics occurring on the edges of the SED gradients. It is possible that detailed coupling between the various spatial scales plays an important role in the evolution and growth of the large scale SED plumes. By making small scale measurements of electric fields, we can help to elucidate the coupling between the physical processes.

4.3 Fixed-bias DC Langmuir Probe (DCP): Traditionally, the DCP has been a Langmuir probe operated at a fixed-bias in the electron saturation region to give high resolution relative electron density measurement [Barjatya and Swenson, 2006]. However, at spacecraft orbital speeds, the magnitude of ion ram current is significantly higher than the ion thermal current. With accurate knowledge of the spacecraft speed and the probe ram cross-section area, a DCP operating in the ion saturation region can give high resolution absolute ion density measurements. An example of both electron and ion density measurements made by the Langmuir probes on the FPMU is shown in Figure 7.

The DICE mission uses two separate spherical DCP sensors operating in the ion saturation region that have a measurement ion density range of 2×10^{9} to 2×10^{13} m^{-3} and a minimum resolution of 3×10^{8} m^{-3}. The two sensors are deployed on separate fiberglass 5 cm long cylindrical booms that will extend into the plasma environment from the top and bottom of the spacecraft along its spin axis (ref. Figure 5). The booms are 3 mm in diameter and support 1 cm diameter spheres. These

spheres are gold-plated and conductive, but the booms themselves are electrically insulated from the plasma environment by static dissipative germanium-coated Kapton tape.

Along each spacecraft's orbital path, spin-stabilized attitude coupled with the DCP deployment geometry results in at least one of the two DCP spheres always facing the velocity vector ram direction (see Figure 6). The use of a spherical probe gives the most uniform ram projected cross-section area for most of the orbital path, with the exception of high polar latitudes. The DCP sensors are biased to -4 VDC to repel electrons and allow for ion ram current measurements during flight. Due to the nature of the orbit and the variation of the ionosphere, the Debye length is expected to vary anywhere between a few mm to upwards of 15 cm. However, due to high spacecraft velocity that far exceeds the local ion mobility, the ion ram current collected by the DCP sensors will not be affected by Debye lengths that are larger than the DICE spacecraft and DCP sensor dimensions. In the nominal operating mode, the measurements from both DCP sensors will be made simultaneously and telemetered at 2 Hz each. Oversampling and decimation of the resultant signal occurs between the distinct telemetry sample points to improve signal to noise.

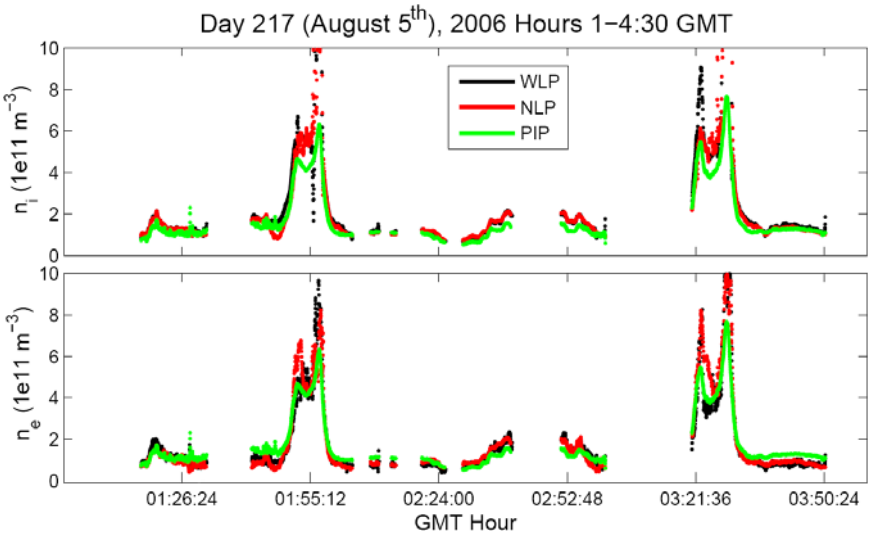

Figure 7. Electron and ion densities observed by FPMU on the ISS over 150 minutes. The peaks are the equatorial anomaly observed over two passes and gaps are due to ISS Ku-band telemetry dropouts. The densities were observed using three different instruments all collocated on the FPMU. The WLP is a spherical Langmuir probe, the NLP is a cylindrical Langmuir probe and the PIP is an impedance probe used to obtain the plasma frequency. The ion densities are computed from the ion saturation current, or ram current, and the projected area of the probes. The electron densities are obtained by fitting to a model of the IV curve for each of the Langmuir probes. As shown in these figures the observed density using these three different probes and five different techniques all agree to within 10%.

5. ORBITAL REQUIREMENTS

The DICE investigation has been designed to be flexible in its ability to accomplish the mission science objectives over a range of expected NSF sponsored LEO CubeSat space mission opportunities. The first general consideration is compliance with the national de-orbit policy. This policy requires de-orbit within 25 years (reference NMI 1700.8, NPR 8715.6, and NSS 1740.14). The DICE mission complies with the de-orbit policy at altitudes up to approximately 630 km. The resultant de- orbit policy altitude constraint is the only practical limiting factor to LEO mission altitude options. The SED plasma enhancements extend over a broad altitude range that includes the plasmapause, however Figure 2 shows that the optimal height for plasma density sampling is between 300 and 600 km, in which the peak SED density values occur. A quasi-circular orbit is preferred, so that the sampling height does not vary significantly, however an elliptical orbit with periapsis of 350 km, and apoapsis of 600 km would be acceptable. The orbital parameters versus science return for the DICE mission are summarized in Table 2.

Orbital inclination is a key consideration in determining mission science return. The primary source region for the SED plasma appears to be in the 12-16 LT region over the USA sector (see Figures 1-4. Therefore, a relatively high inclination orbit with a relatively slow precession is required to map the formation and evolution of SED. A 12-16 LT sun-synchronous orbit would be optimal as it would ensure sampling of the SED and bulge every time they occur, and it does not duplicate the DMSP measurements near 18 LT. If a 12-16 LT sun synchronous orbit is not available, a mission with an inclination of 55º or greater is needed for full science return. For example, an orbit of 600 km and 55º would have a precession rate of 4°

per day, or 16 minutes LT per day. This provides 15 days of continuous data collection in the optimal 12-16 LT range every 45 days. Relatively little is known about the LT and longitude variation of the low-latitude electric fields. Therefore any inclination or LT will yield valuable new information about them.

Table 2. DICE Acceptable Orbits

Mission/Science Orbit Applicability		
Altitude:		**350-600 km**
Inclin:	**Sun Sync**	Optimal
	55-85°	Very Good
	0-55°	Good
Optimal = Optimal science, Very Good = Full science, Good = Reduced science		

6. TECHNICAL APPROACH

Each DICE spacecraft follows a CubeSat 1.5U form factor, divided roughly into payload, electronics, communications, and attitude control sections. A key design element in the DICE spacecraft is the use of flight-proven industrial-grade components and design approaches from the spaceflight-proven CubeSat community. This strategy reduces the design effort and mission cost. Complementary to the use of low cost flight-proven hardware, the complete spacecraft will be rigorously tested and qualified for spaceflight. The science payload (EFP and DCP) is based on instrumentation that USU/SDL has flown for over 20 years on multiple space flight missions, including most recently FPMU [2005] and the Tropical Storm [2007] and EQUIS II [2005] sounding rocket programs.

The PEARL platform developed by SDL is an excellent fit for the DICE mission, providing all of the necessary scientific, power, data processing, communications, and attitude control resources. The PEARL mission is a 1.5U CubeSat program, supported by Air Force and internal USU/SDL funding. The PEARL and follow-on DICE spacecraft designs rely heavily on flight-proven CubeSat community components, including components from Pumpkin Inc., Clyde Space Ltd., Honeywell, NovAtel, and Analog Devices. The DICE spacecraft capabilities overview is given in Table 3. The current mission design contingency and margin levels are summarized in Table 4.

Figure 8 depicts the spacecraft subsystems and block diagram. On DICE, the very-low-power FM430 processor card and Salvo operating system provide the C&DH capabilities. Power is generated from solar panels attached to the long, outer faces of the spacecraft providing power at all times while the spacecraft is not in eclipse. Power is stored in a high-energy-density Lithium Polymer battery. Embedded torque coils provide periodic momentum dumping and attitude control capability. Attitude determination and navigation sensors include sun sensors, a magnetometer, horizon sensor, micro-electromechanical system (MEMS) gyros, and a miniature GPS receiver. The use of the GPS is kept to a minimum (duty-cycled) to reduce orbital average power. A UHF transceiver supports data rates up to 1.50 Mbp/s downlink and 19.20 kbp/s uplink (see Section 8 below).

7. TRACEABILITY TO MISSION/SCIENCE REQUIREMENTS

The DICE spacecraft requirements are driven by mission requirements (Table 1). The mission to spacecraft traceability is shown in Table 5. All spacecraft requirements are met with margin (Table 4).

Table 3. DICE Mission Spacecraft Overview

Mass / Volume	1.42 kg / 1814 cm^3
Power Usage	1.13 W EOL (OAP)
Power Gen	1.69 W EOL (OAP)
Power Storage	1.25 A-hr
Attitude Control	<5.00°, 1σ, spin-stabilized
Processor	1.5 MIPS, RTOS
Attitude Knowledge	<0.70°, 1σ, real-time <0.20°, 1σ, ground
Communications *(see Section 8)*	1.5 Mbp/s down. 19.20 kbp/s up
EOL = End of Life, OAP = Orbit Average Power	

Table 4. DICE Mission Spacecraft Design Contingency and Margin

Category	Available	Units	Assigned Contingency	CBE + Contingency	Margin
Mass Budget	1.50	kg	15%	1.42	6%
EOL Load Power Generation Budget	1.69	W	20%	1.13	94%
CPU Processing Budget	1.5	MIPS	20%	1.2	25%
Memory Budget, CPU ROM	48,000	Kbytes	20%	27,196.00	76%
Memory Budget, CPU RAM	10,000	Kbytes	20%	8,558.00	17%
Data RAM Budget	2,000	Mbytes	20%	10.50	18948%
Attitude Control	10.00	°	20%	<5.00	100%
Attitude Knowledge (real-time)	1.0	°	20%	<0.70	43%
Att. Knowledge (post processed)	1.0	°	20%	<0.20*	400%
Link Budget, Uplink	4.00	dB		19.30**	15.30dB
Link Budget, Downlink	4.00	dB		5.93**	1.93dB

CBE = Current Best Estimate, EOL = End of Life, DOD = Depth of Discharge

Contingency is resource allocation above CBE that then defines the maximum expected value for the resource. Margin is the difference between the maximum possible resource value and maximum expected resource value. *In combination with science $\boldsymbol{v} \times \boldsymbol{B}$ electric field data, **Given a 675 km orbit

Table 5. Traceability to mission/science requirements

Mission Requirements	Spacecraft Requirements	Ground System Requirements	Operations Requirements
Lifetime ≥ 6 months	Lifetime ≥ 6 months	Lifetime ≥ 6 months	Operations ≥ 6 mos
Launch via P-POD	≤ 1.5 kg mass, unpowered	None	Launched unpowered
Spin-stabilized ≥ 0.8 Hz	Spin-stabilized ADCS	None (control autonomous)	None (control autonomous)
S/C spin axis to geodetic axis to ≤ 10º (1σ)	≤ 10º (1σ) attitude control	None (control autonomous)	None (control autonomous)
S/C spin ≤ 1º (1σ) about principal spin axis	Mass balance for spin axis <1º (1σ) about principal axis	None	Monitor spin axis telemetry
Constellation synch ≤ 1 s	Time synch ≤ 0.5 s	Time synch ≤ 1 s	Time synch ≤ 1 s
S/C delV of ≤ 50 km/month	S/C separation of 6 mm/s	None	Monitor spacing
Downlink rate ≥ 31 Mbits/day for science data	On-board storage ≥ 70 Mbits Downlink ≥ 36.5 Mbits/day (includes HK & ADCS data)	Daily contacts with downlink ≥ 36.5 Mbits	Daily contacts with downlink ≥ 36.5 Mbits

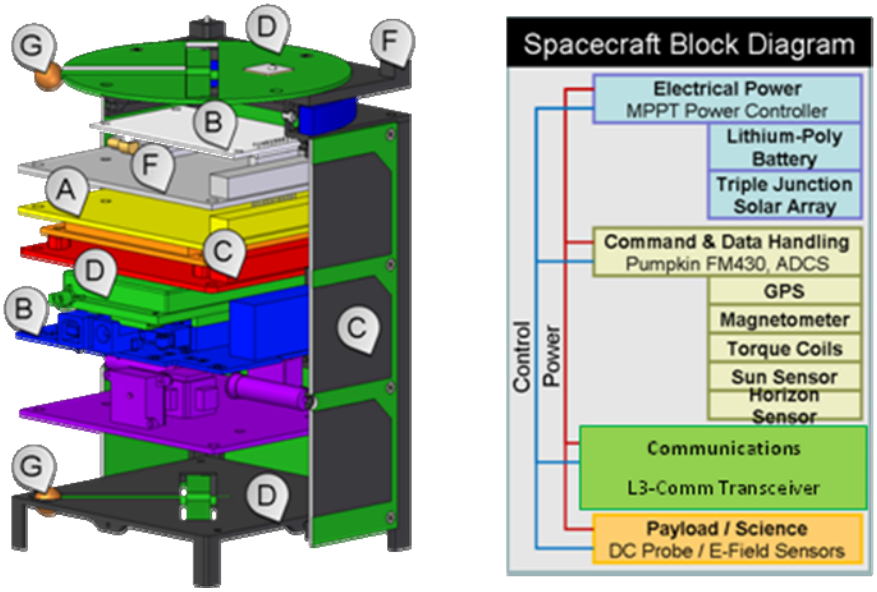

Figure 8. Spacecraft subsystems & block diagram (see Table 6 for corresponding lettering and sub-system details).

8. DICE TELEMETRY CONCEPT

The DICE mission is not using traditional CubeSat amateur radio systems and frequencies, but is instead using government radio bands and high speed downlink rates that are consistent with a NSF funded mission. A half-duplex UHF modem developed for DICE by L3-Communications provides a 1.5 Mbit/s downlink and a 19.2 kbit/s uplink. Each DICE modem will be continuously listening for ground station commands, which will switch it into transmit mode for a short period of time after which it returns to listen mode. Therefore, the spacecraft modem is fully controlled by the ground station and the spacecraft cannot autonomously turn on the modem's transmitter. All Space-to-Earth communications are responses to ground station commands that request data packets from the modem. Both spacecraft will use identical up- and downlink frequencies but will have unique logical addresses decoded by the modem. The ground stations are proposed to be at Wallops Island on the east coast and/or at SRI on the west coast. The L3 modem will be connected to a DICE program-supplied computer, which will act as a primary mission operations center and provide connection via the internet to the secondary mission operations and primary science operations center located in Logan, Utah. It is expected that during normal conditions the entire mission will be controlled over the internet from a combined mission and science center at the Space Dynamics Laboratory.

9. STUDENT PARTICIPATION

A majority of the DICE mission is being developed and implemented by graduate and undergraduate students with professional staff serving as mentors to ensure the program is progressing successfully and meeting requirements. The DICE mission is an excellent opportunity for engineering and physics students to become closely involved with space science and hardware/software design. Student jobs have been created, currently employing 7 under-graduates and 5 graduates at USU (6 in mechanical and aerospace engineering, 2 in civil engineering, and 4 electrical engineering students). More jobs will be created as the mission progresses. These will involve opportunities in data handling, quality control, validation, and analysis. Aerospace engineering students are producing the spacecraft and instrument design drawings, developing hardware and software interface documents, performing stability, worst-case, and Monte Carlo engineering analyses, integrating and testing hardware, and calibrating the instruments. They are developing mission operations plans, including ground station operations, and preparing the spacecraft for launch. Physics students will play a major role in the calibration of the instrument, analysis and dissemination of the science products, and publication of the scientific findings. ASTRA will be the public interface for the DICE data, and students are expected to play a large role in the DICE data center. In addition to hands-on work prior to launch, the operational mission will provide material for classes that will serve to motivate students with regard to science, technology, engineering, and mathematics. Students have been the main contributors and participants during regular DICE program status meetings, telecons, technical interchange meetings, and major reviews.

8. REFERENCES

1. Anderson, D., A. Anghel, K. Yumoto, M. Ishitsuka, and E. Kudeki (2002), Estimating

2. daytime vertical ExB drift velocities in the equatorial F-region using ground-based magnetometer observations, Geophys. Res. Lett., 29(12), 1596, doi:10.1029/2001GL014562.

3. Anderson, D., A. Anghel, J. Chau, and O. Veliz (2004), Daytime vertical ExB drift velocities inferred from ground-based magnetometer observations at low latitudes, Space Weather, 2, S11001, doi:10.1029/2004SW000095.

4. Anderson, D., A. Anghel, J. L. Chau, and K. Yumoto (2006), Global, low-latitude, vertical ExB drift velocities inferred from daytime magnetometer observations, Space Weather, 4, S08003, doi:10.1029/2005SW000193.

5. Barjatya, A. and C.M. Swenson (2006), Observations of triboelectric charging effects on Langmuir type probes in dusty plasma, Accepted for publication in J. Geophys. Res

6. Basu, Su., S. Basu,J. J. Makela,R. E. Sheehan,E. MacKenzie,P. Doherty,

7. J. W. Wright,M. J. Keskinen,D. Pallamraju,L. J. Paxton,and F. T. Berkey (2005), Two components of ionospheric plasma structuring at midlatitudes observed during the large magnetic storm of October 30, 2003, Geophys. Res. Lett., 32, L12S06, doi:10.1029/2004GL021669.

8. Bust, G.S, T.W. Garner, and T. L. Gaussiran II, Ionospheric Data Assimilation Three Dimensional (IDA3D): A Global, Multi-Sensor, Electron Density Specification Algorithm, J. Geophys. Research,109, A11312, doi:10.1029/2003JA010234, 2004.

9. Bust, G. S., G. Crowley, T. W. Garner, T. L. Gaussiran II, R. W. Meggs, C. N. Mitchell, P. S. J. Spencer, P. Yin, and B. Zapfe (2007) ,Four Dimensional GPS Imaging of Space-Weather Storms, Space Weather, 5, S02003, doi:10.1029/2006SW000237.

10. Bust, G.S., (2008), Mapping the Time-varying Distribution of High Altitude Plasma During Storms, Accepted for publication in Chapman Book Series "Mid-latitude Ionospheric Dynamics and Disturbances"

11. Bust, G. S., N. Curtis, A. Reynolds, and G. Crowley (2008a), Equatorial and Mid-latitude Plasma Redistribution During Storms, submitted to J. Geophys. Res.

12. Bust, G.S., N. Curtis, A. Reynolds, G. Crowley, and S. Datta-Barua (2008b), Storm-time distribution of plasmaspheric electron densities, in preparation

13. Bust, G.S., and G. Crowley, Tracking of Polar Cap Ionospheric Patches using Data Assimilation, J. Geophys. Res., in press, 2006.

14. Bust, G.S., S. Datta-Barua, N. Curtis, A. Reynolds, and G. Crowley (2008c), Storm induced post sunset plasma density enhancements, submitted to J. Geophys. Res.

15. Bust, G.S, et al., Ionospheric Data Assimilation Three Dimensional (IDA3D): A Global Multi-Sensor Electron Density Specification Algorithm, J. Geophys. Research,109, doi:10.1029/2003 JA010234, 2004.

16. Coker, C., Bust, G.S., et al., High-latitude Plasma Structure and Scintillation, Radio Science, 39,doi:10.1029/2002RS002833, 2004.

17. Crowley, G., and M.C. Kelley, Storm-time Penetration E-fields at Jicamarca and Comparisons with the TIMEGCM First-

Principles Model, submitted to J. Geophys. Res., 2008.

18. Crowley, G., C. Hackert, R. R. Meier, D. J. Strickland, L. J. Paxton, X. Pi, A. Manucci, A. Christensen, D. Morrison, G. Bust, R. G. Roble, N. Curtis, G. Wene, Global Thermosphere-Ionosphere Response to Onset of November 20, 2003 Magnetic Storm, J. Geophys. Res., 111, A10S18, doi:10.1029/2005JA011518, 2006

19. Crowley, G. and C. Hackert, Quantifying the temporal variability of the high latitude electric field using AMIE, GRL, 28, 2783-2786, 2001

20. Coster, A. J., J. Foster, and P. Erickson, Monitoring the Ionosphere with GPS: Space Weather, GPS World, 14(5), 42-49, 2003.

21. Dehel, T., "Solar Flares Hit Earth – WAAS Bends But Does Not Break", 2004.

22. Erickson, P.J., J.C. Foster, and J.M. Holt (2002), Inferred electric field variability in the polarization jet from Millstone Hill E region coherent scatter observations, Radio Sci., 37, doi:10.1029/2000RS002531

23. Foster, J. C. (1993), Storm time plasma transport at middle and high latitudes, J. Geophys. Res., 98, 1675.

24. Foster, J. C., A. J. Coster, P. J. Erickson, J. Goldstein, and F. J. Rich, Ionospheric Signatures of Plasmaspheric Tails, Geophys. Res. Lett., 29(13), 10.1029/2002GL015067, 2002.

25. Foster, J. C., and H. B. Vo, Average characteristics and activity dependence of the subauroral polarization stream, J. Geophys. Res., 107(A12), 1475, doi:10.1029/2002JA009409, 2002.

26. Foster J.C., P. J. Erickson, F.D. Lind, and W. Rideout (2004), Millstone Hill coherent-scatter radar observations of electric field variability in the sub-auroral polarization stream, Geophys. Res. Lett., 31, L21803, doi:10.1029/2004GL021271

27. Foster, J. C., and W. Rideout (2005), Midlatitude TEC enhancements during the October 2003 superstorm, Geophys. Res. Lett., 32, L12S04, 10.1029/2004GL021719

28. Foster, J. C., and A.J. Coster, (2007), Conjugate localalized enhancement of total electron content at low latitudes in the American sector, Journal of Atmospheric and Solar-Terrestrial Physics 69 (2007) 1241–1252, doi:10.1016/j.jastp.2006.09.012

29. Foster, J.C., W. Rideout, B. Sandel, W.T. Forrester, and F.J. Rich, (2007), On the relationship of SAPS to storm-enhanced density, Journal of Atmospheric and Solar-Terrestrial Physics 69 (2007) 303–313, doi:10.1016/j.jastp.2006.07.021

30. Klobuchar, J. A., J. Aarons, and H. H. Hosseinich (1968), Midlatitude nighttime total electron content behavior during magnetically disturbed periods, J. Geophys. Res., 73, 7530–7534.

31. Klobuchar, J. A., M. Mendillo, F. L. Smith III, R. B. Fritz, A. V. Da Rosa, M. J. Davis, P. C. Yuen, T. H. Roelofs, K. C. Yeh, and B. J. Flaherty (1971), Ionospheric storm of March 8, 1970, J. Geophys. Res., 76, 6202–6207.

32. Ledvina, B. M., J.J. Makela, and P.M. Kintner, "First observations of intense GPS L1 amplitude scintillations at midlatitude,"Geophys. Res. Lett., 29(14), 1659, doi:10.1029/2002GL014770, 2002.

33. Mannucci, Tsurutani, Abdu, Gonzales, Komjathy, IIjima, Crowley and Anderson, "Superposed Epoch Analysis Of The Ionospheric Response To Four Intense

Geomagnetic Storms", submitted to J. Geophys. Res., August 2007

34. Mendillo, M. (2006), Storms in the ionosphere: Patterns and processes for total electron content, Rev. Geophys., 44, RG4001, doi:10.1029/2005RG000193.

35. NWSP (2006), Report of Assessment Committee for the National Space Weather Program, FCM-R24-2006, Office of Federal Coordinator for Meteorological Services and Supporting Research (OFCM), Silver Spring MD.

36. Skone, S., M. El-Gizawy, and S. M. Shrestha, (2004), Analysis of differential GPS performance for marine users during solar maximum, Radio Sci., 39,RS1S17, doi:1029/2002RS002884

37. Sojka, J. J., D. Rice, J. V. Eccles, F. T. Berkey, P. Kintner, and W. Denig (2004), Understanding midlatitude spaceweather: Storm impacts observed at Bear Lake Observatory on 31 March 2001, Space Weather, 2, S10006,doi:10.1029/2004SW000086.

38. Sparks, L., A. Komjathy, and A. J. Mannucci (2004), Sudden ionospheric delay decorrelation and its impact on the Wide Area Augmentation System (WAAS), Radio Sci., 39, RS1S13, doi:10.1029/2002RS002845.

39. Watermann, J., G. S. Bust, et al., Mapping plasma structures in the high-latitude ionosphere using beacon satellite, incoherent scatter radar and ground-based magnetometer observations, 45(1), Annals of Geophysics, 2002.

40. Yin, P., C.N. Mitchell, and G.S. Bust, Observations of the F region height redistribution in the stormtime ionosphere over Europe and the USA using GPS ,Geophys. Res. Lett.,submitted, 2006.

Acknowledgments: The authors wish to thank all of the USU Staff and students that have helped with the design and building of the DICE instruments and spacecraft. The DICE team would like to acknowledge support from NSF Grant 0838059.